

Supplementary Materials for:

Factors Influencing the Surface Functionalization of Citrate Stabilized Gold Nanoparticles with Cysteamine, 3-Mercaptopropionic acid or L-Selenocystine for Sensor Applications

Results

Characterization of Citrate-Stabilized AuNPs

The comparison of the UV-vis spectroscopy data and physical appearance of the AuNP solutions, purchased and in-house synthesized, is depicted in Figure S1.

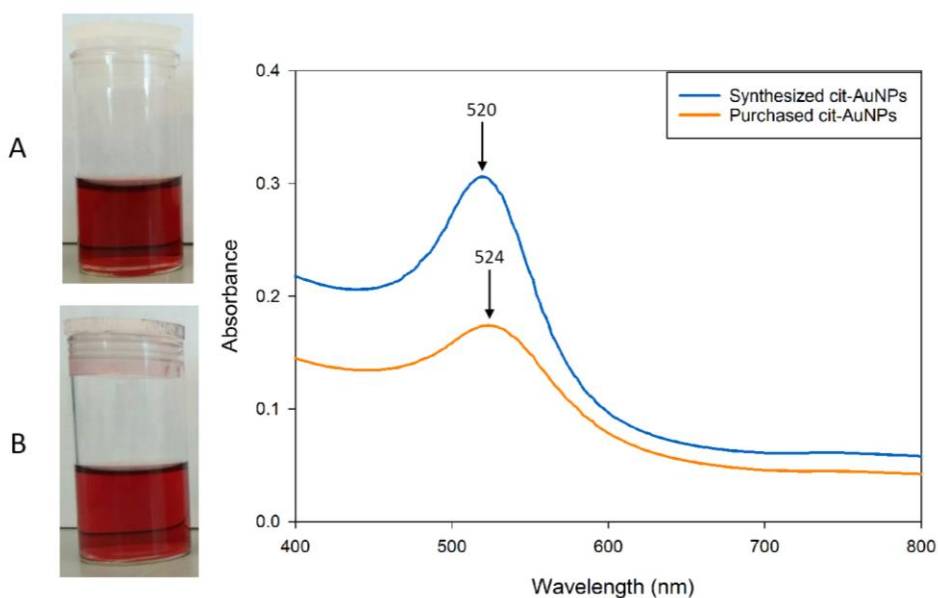


Figure S1. Comparison of colloidal solutions and UV-vis extinction spectra of citrate stabilized AuNPs, A) synthesized solution with absorbance maximum at 520 nm, and B) purchased solution with a maximum at 524 nm.

TEM was initially used to image the nanoparticles with resultant measurements indicating that the purchased nanoparticles have an average diameter of 7.3 ± 1.2 nm (Figure S2), and the synthesized nanoparticles have an average diameter of 13.8 ± 1.2 nm (Figure S3).

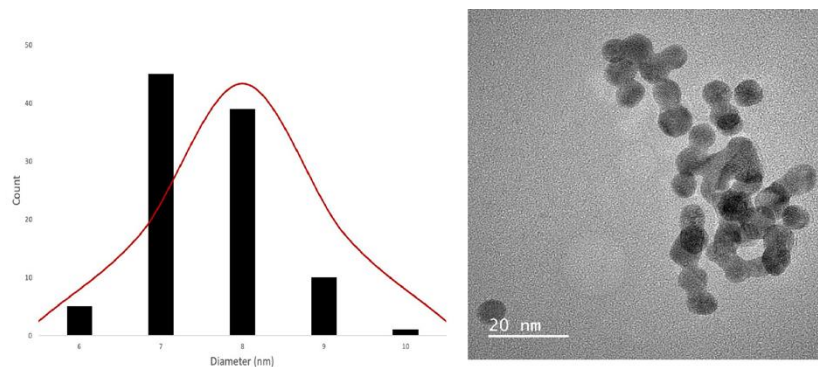


Figure S2. Histogram of the particle diameter of purchased Cit-AuNPs. The average diameter was calculated for 100 nanoparticles using ImageJ software.

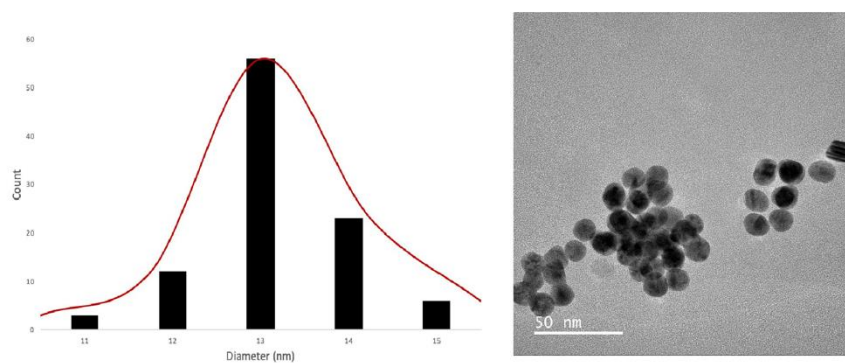


Figure S3. Histogram of the particle diameter of synthesized Cit-AuNPs. The average diameter was calculated for 100 nanoparticles using ImageJ software.

The $^1\text{H-NMR}$ spectra acquired to compare the composition of the two types of AuNPs are shown in Figure S4. Additionally, the spectrum of trisodium citrate is provided in support of the identification of the peaks present in the spectra of the synthesized and purchased AuNP solutions (Figure S5).

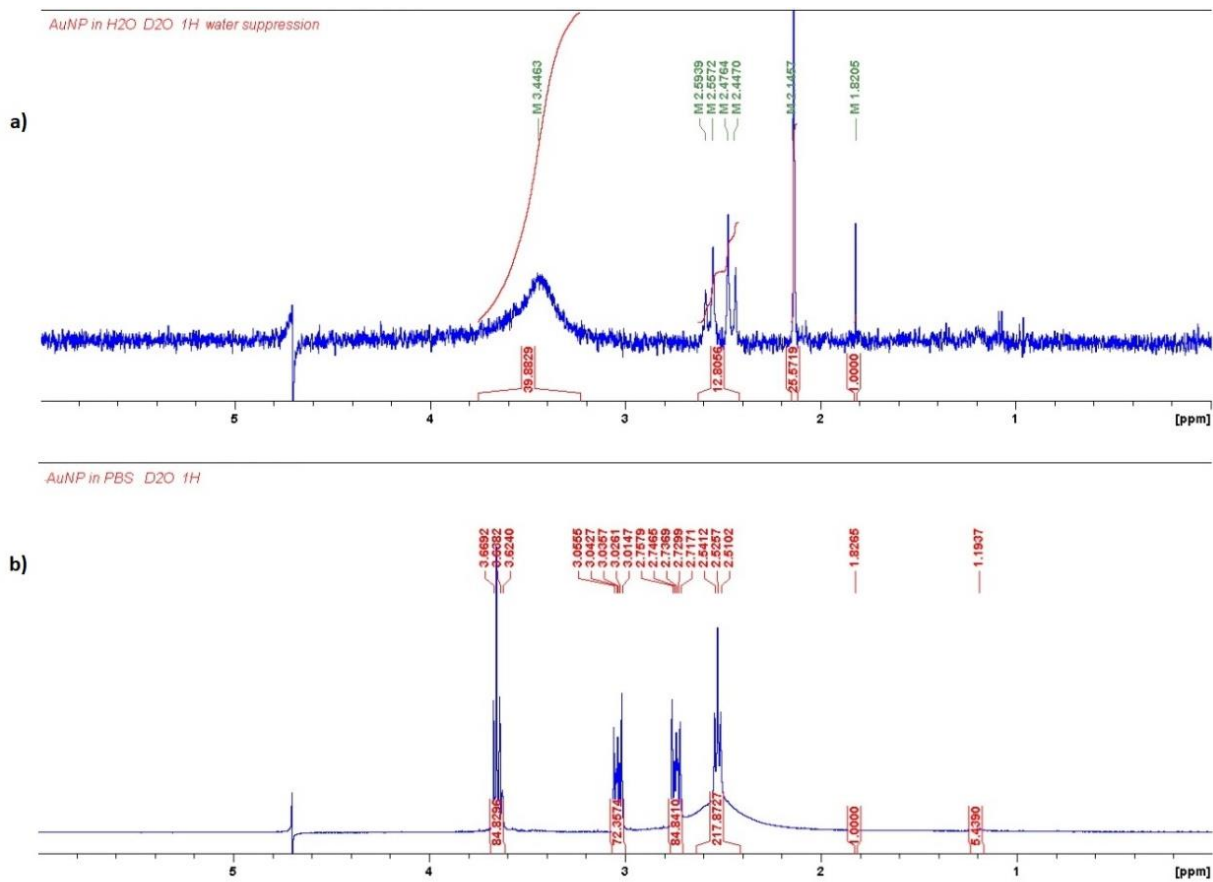


Figure S4. 400 MHz ^1H NMR spectra of a) synthesized Cit-AuNP, and b) purchased Cit-AuNP.

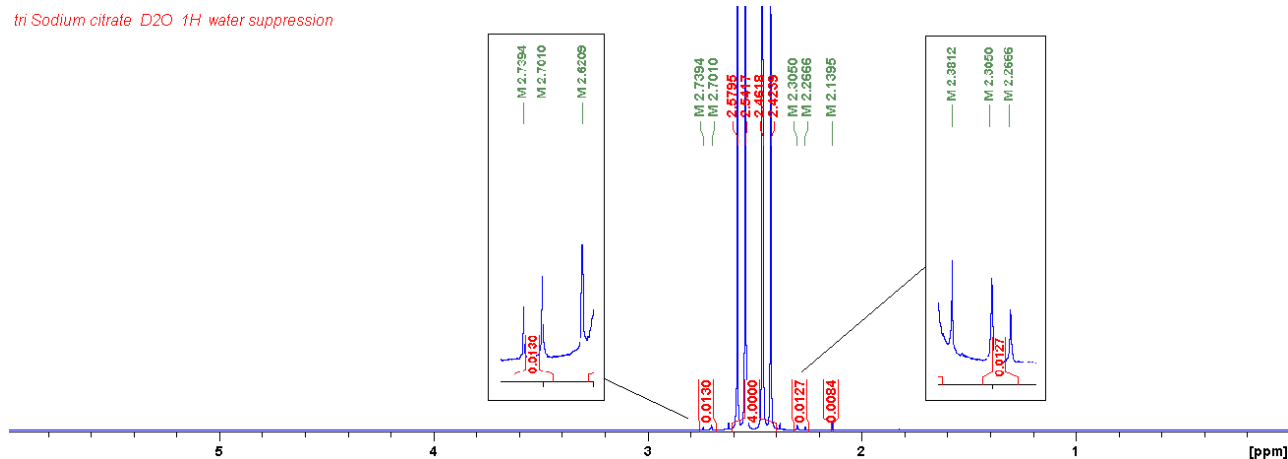


Figure S5. 400 MHz ^1H NMR spectra of trisodium citrate dihydrate.

ATR-FTIR spectroscopy measurements were performed to confirm the formation of citrate stabilized AuNPs and study their composition, and the results are depicted in Figure S6 and Table S1. The spectrum of trisodium citrate dihydrate was also obtained as a reference (Figure S7).

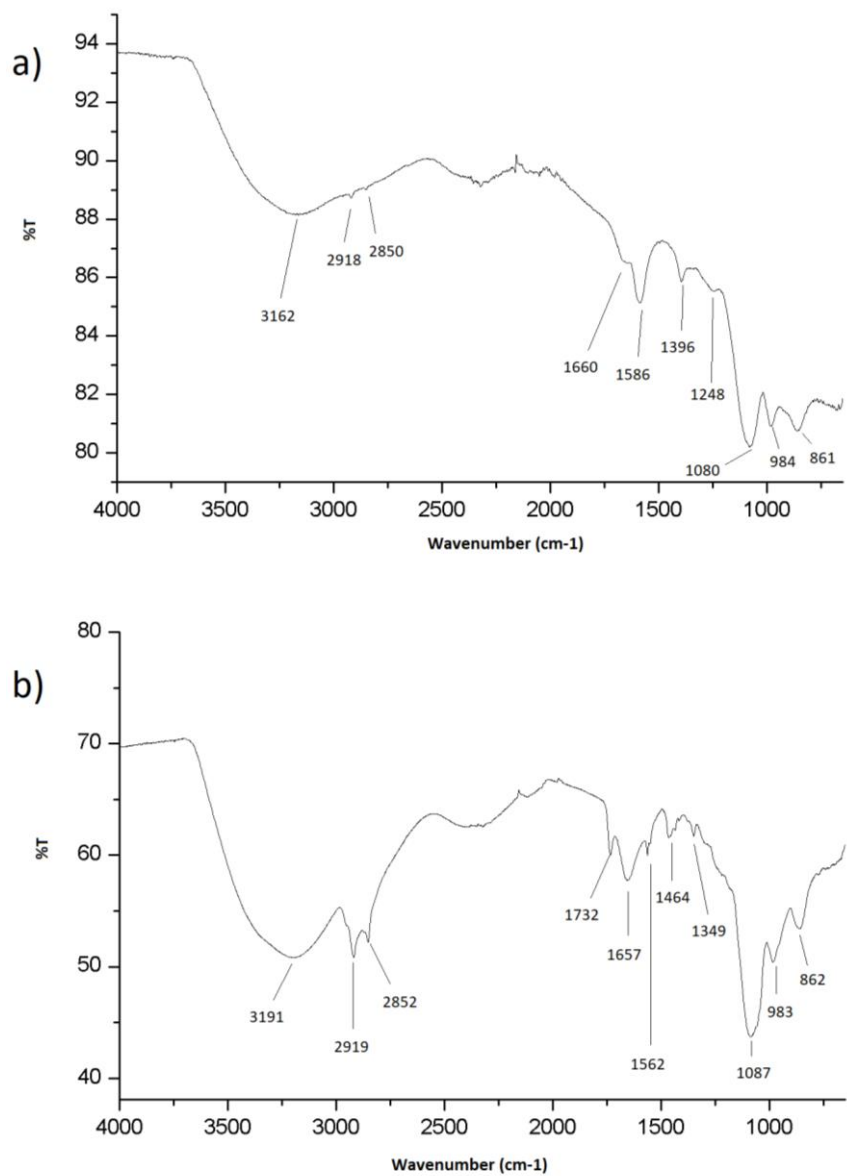


Figure S6. ATR-IR spectra of citrate stabilized a) synthesized AuNPs, and b) purchased AuNPs.

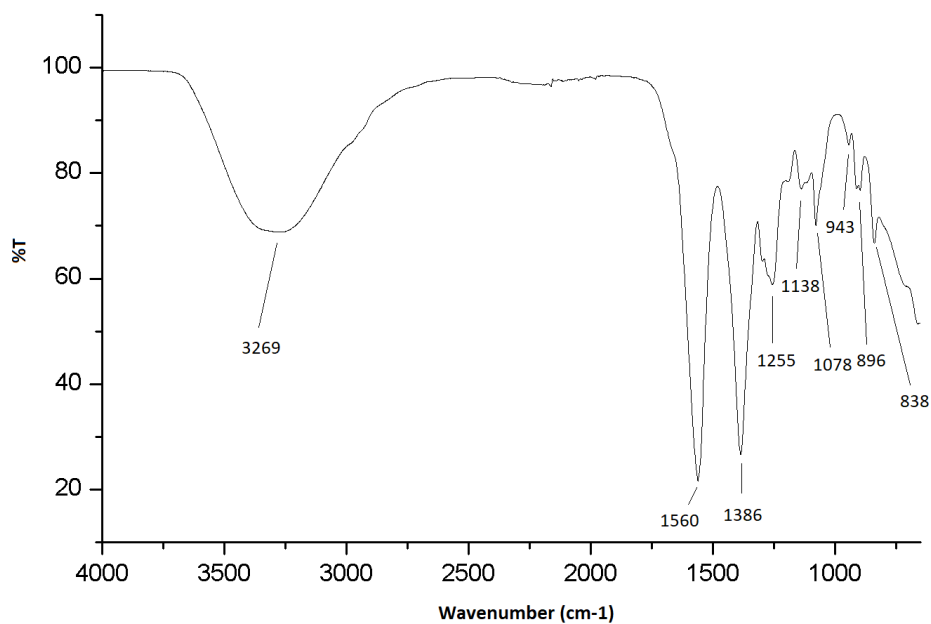


Figure S7. ATR-IR spectrum of trisodium citrate dihydrate.

Table S1. ATR-FTIR data for synthesized, purchased Cit-AuNPs and trisodium citrate.

Wavenumber (cm ⁻¹)			
Trisodium citrate dihydrate	Synthesized AuNPs	Purchased AuNPs	Peak Assignment
3269	3162	3191	$\nu(\text{O-H})_{\text{COOH}}$
	2918	2919	$\nu(\text{C-H})$
	2850	2852	$\nu(\text{C-H})$
		1732	$\nu(\text{C=O})$
	1660	1657	$\nu_{\text{asy}}(\text{COO}^-)$
1560	1586	1562	$\nu_{\text{asy}}(\text{COO}^-)$
		1464	$\nu_{\text{sym}}(\text{COO}^-)$
1386	1396	1349	$\nu(\text{COO}^-)$
1255	1248		$\nu_{\text{asy}}(\text{C-O})$
1138			$\nu(\text{C-O})_{\text{alch}}$
1078	1080	1087	$\nu_{\text{asy}}(\text{C-O})_{\text{alch}}$
943	984	983	$\delta(\text{C-H})$
896	861	862	$\delta(\text{C-H})$
838			$\rho(\text{C-H})$

Optimization of the Conditions for the Functionalization of the Citrate-Stabilized AuNPs

A summary of the optimized conditions for the functionalization and purification of the AuNPs is presented below (Table S2).

Table S2. Summary of the optimized conditions followed for the functionalization of citrate stabilized AuNPs with Cys, 3-MPA and SeCyst.

Parameter	Optimal condition
Dissolution medium	Deionized water
pH	10
Functionalizing agent : AuNPs ratio	1:2
Purification protocol	Centrifugation at 13,200 g for 40 min with phosphate buffer (pH 7.7)

Effect of pH on the Functionalization

In order to prevent aggregation, the experiments were performed in HEPES buffer adjusted to pH 7.4. Both thiol compounds showed good stability indicated by UV-visible spectroscopy, although the SPR band had slightly broadened and there was a very small bathochromic or red shift of the peak maximum, the band shape remained unchanged after overnight incubation (Figure S8).

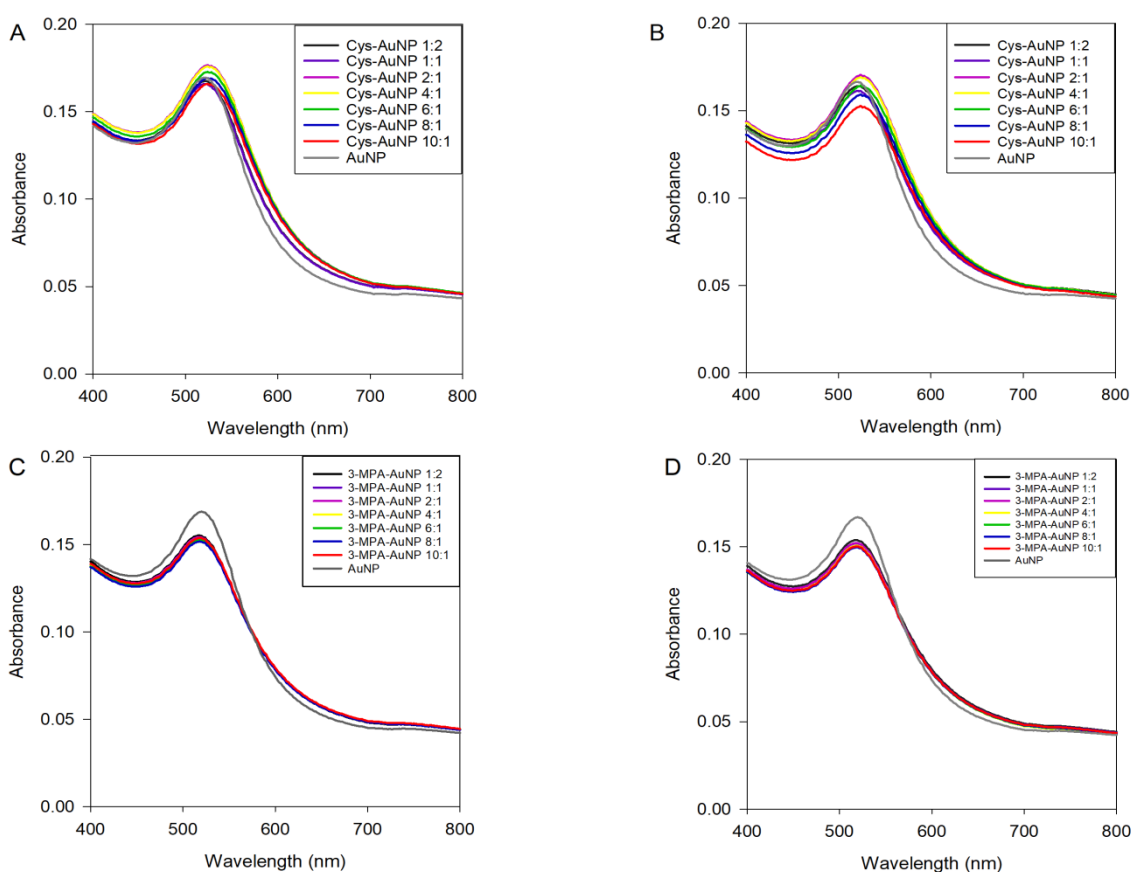


Figure S8. UV-vis spectra for stability assessment of A) Cys-AuNP after 2 h incubation, B) Cys-AuNP after overnight incubation, C) 3-MPA-AuNP after 2 h incubation, and D) 3-MPA-AuNP after overnight incubation, in HEPES buffer with adjusted pH 7.4, at various ratios.

UV-vis spectroscopy data obtained for the SeCyst functionalized AuNPs in HEPES buffer and the stability of their respective SPR bands after 2 h and overnight incubation is demonstrated in Figure S9.

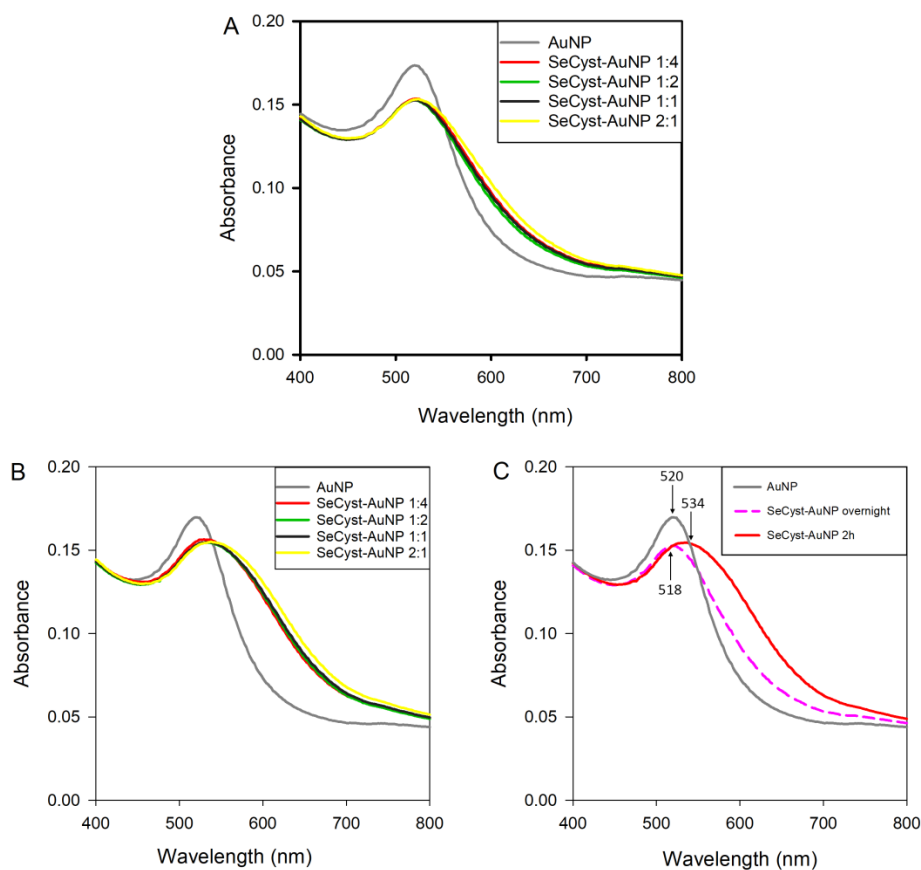


Figure S9. UV-vis spectra of A) SeCyst-AuNP after 2 h incubation, and B) SeCyst-AuNP after overnight incubation in HEPES buffer adjusted at pH 7.4, at the various ratios. C) Comparison of the UV-vis spectrum of SeCyst-AuNP after 2 h (dashed line), and SeCyst-AuNP overnight (bold line).

The stability of the SeCyst functionalized AuNPs in phosphate buffer over a period of six days is given in Figure S10. During this incubation time, the band maximum red shifted, and peak broadening was observed.

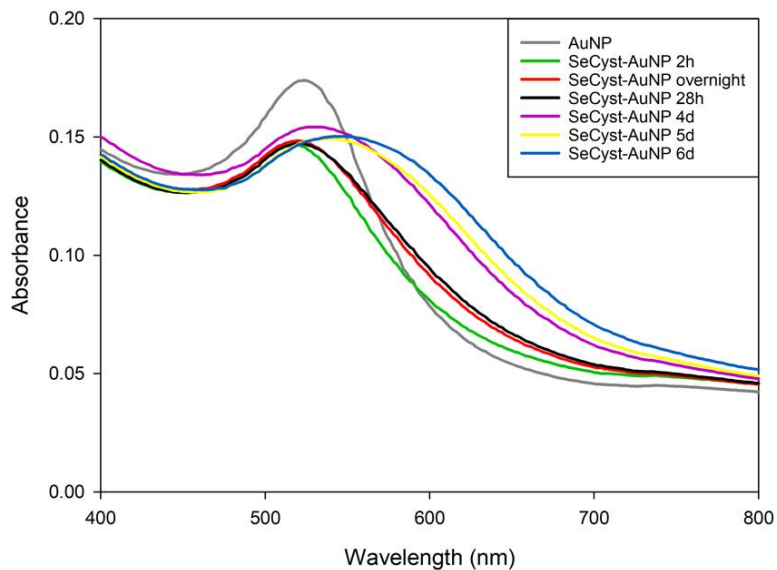


Figure S10. UV-vis spectrum of SeCyst-AuNP (1:2 ratio) in phosphate buffer pH 7.7 over a period of 6 days.

Changes in the UV-vis spectra of the AuNPs functionalized with Cys and 3-MPA in deionized water at different ratios, after 2 hours and 4 days are depicted in Figure S11. Stability of Cys-AuNPs was confirmed over the incubation time of 4 days, while 3-MPA-AuNPs demonstrated both physical (precipitation and colour change) and peak broadening at higher ratios.

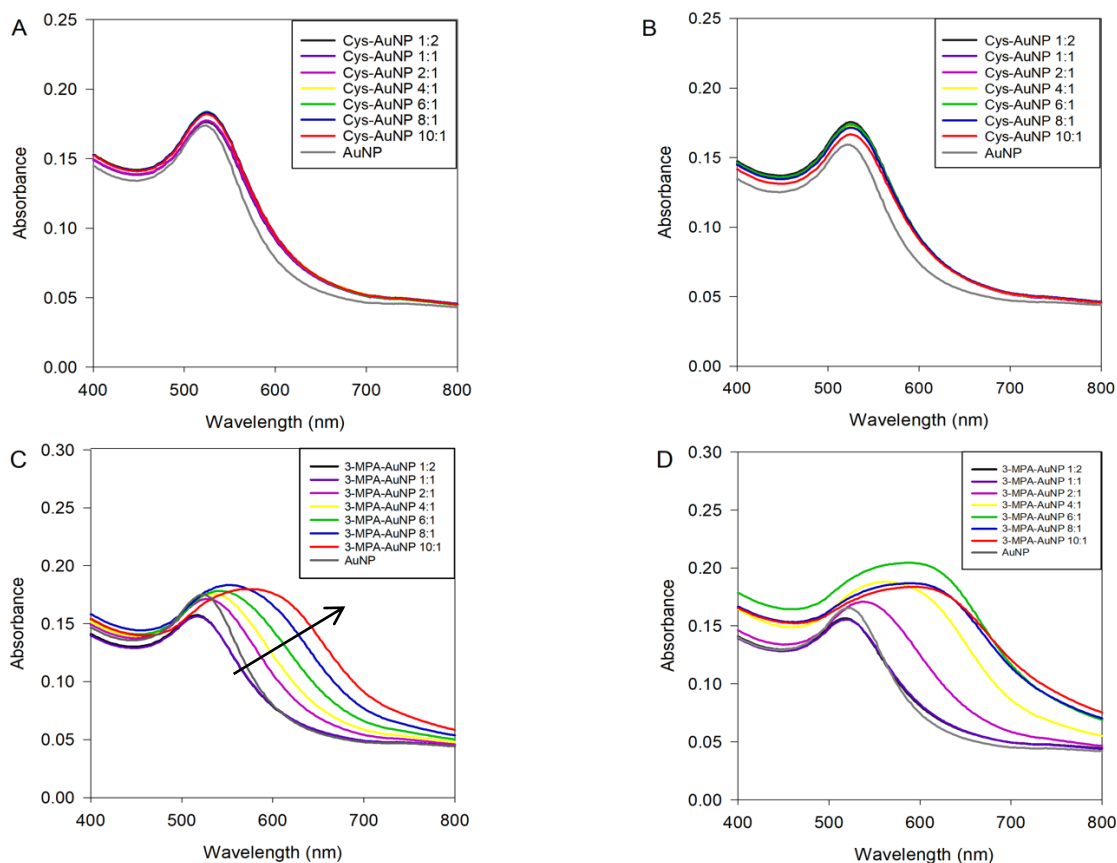


Figure S11. UV-vis spectra for stability assessment of A) Cys-AuNP after 2 h incubation, B) Cys-AuNP after 4 d incubation, C) 3-MPA-AuNP after 2 h incubation, and D) 3-MPA-AuNP after 4 d incubation, in deionized water, at various ratios.

Characterization of Capped-AuNPs by FTIR

The peak assignments for the cysteamine containing samples are presented in Table S3. The ATR-FTIR spectra for the cysteamine functionalized AuNP solutions, synthesized and purchased are given in Figure S12. The spectrum of cysteamine solution (pH 5.9) without pH adjustment was also obtained as a reference for the $\nu(\text{S-H})$ stretching vibrational mode, which is identified at 2562 cm^{-1} (Figure S12D).

Table S3. Peak identification and comparison of the data obtained by ATR-FTIR analysis for the samples containing cysteamine.

Wavenumber (cm^{-1})			Peak assignment
cysteamine (0.256 mM, pH 10.8)	Cys-AuNP synthesized	Cys-AuNP purchased	
3344	3224	3188	$\nu(\text{O-H})$
2922	2924		$\nu(\text{C-H})$
2850			$\nu(\text{C=O})$

	1664	1645	$\nu_{\text{asy}}(\text{COO}^-)$
1588	1583		$\nu(\text{C=O}), \nu(\text{N-H})$
1438	1392		$\delta(\text{C-H})$
1233		1246	$\nu_{\text{asy}}(\text{C-O})$
1143			$\nu(\text{C-N})$
	1060	1059	$\nu_{\text{asy}}(\text{C-O})$
	975	976	$\delta(\text{C-H})$
878	839	858	$\delta(\text{C-H})$
700	672	653	$\nu(\text{C-S})$

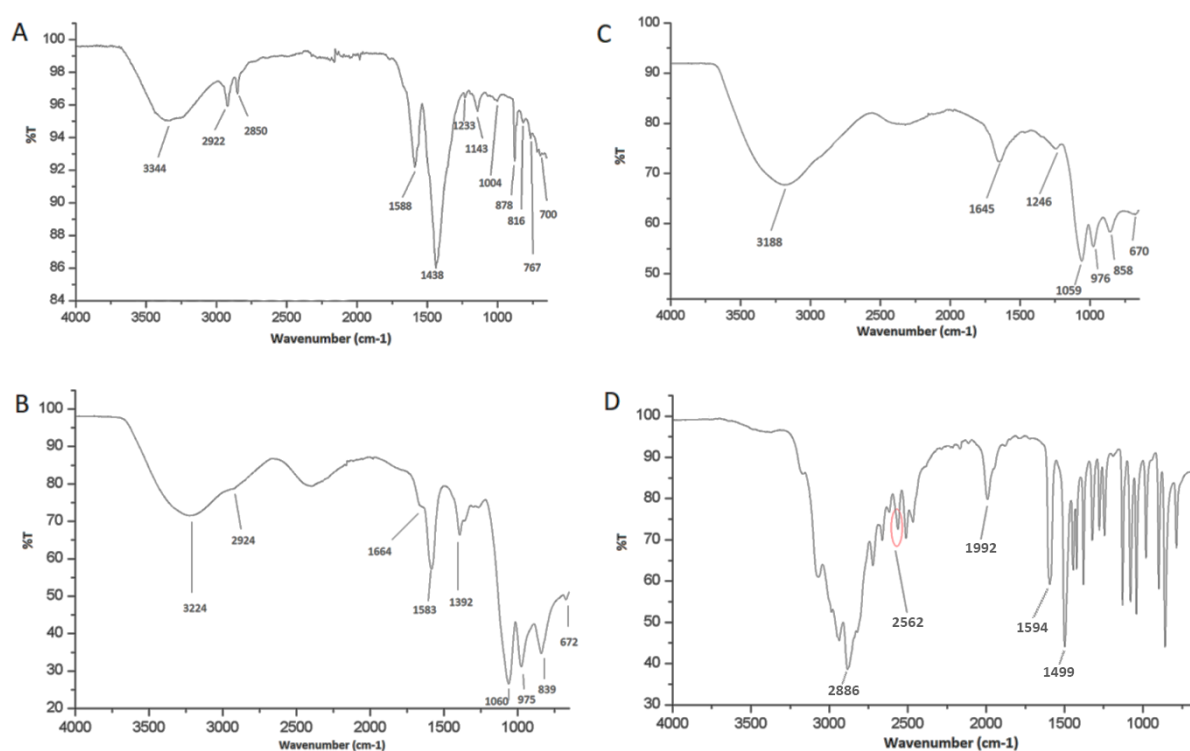


Figure S12. ATR-FTIR spectra of A) cysteamine solution (pH 10.8), B) Cys-AuNP synthesized, C) Cys-AuNP purchased, and D) cysteamine solution (pH 5.9).

The peak assignments for the 3-MPA samples are presented in Table S4. The ATR-FTIR spectra for the 3-MPA functionalized AuNP solutions, synthesized and purchased are shown in Figure S13. The spectrum of 3-MPA solution (pH 4.1) without pH adjustment was also obtained as a reference for the $\nu(\text{S-H})$ stretching vibrational mode, which is identified at 2567 cm^{-1} (Figure S13D).

Table S4. Peak identification and comparison of the data obtained by ATR-FTIR analysis for the samples containing 3-mercaptopropionic acid.

Wavenumber (cm ⁻¹)			Peak assignment
3-mercaptopropionic acid (0.256 mM, pH 10.95)	3-MPA-AuNP synthesized	3-MPA-AuNP purchased	
3186	3177	3144	$\nu(\text{O-H})$
2920	2924		$\nu(\text{C-H})$
2850			$\nu(\text{C-H})$
1654	1656	1642	$\nu_{\text{asy}}(\text{COO}^-)$
1549	1585	1566	$\nu(\text{C=O}), \nu(\text{N-H})$
1400	1393	1389	$\delta(\text{C-H})$
	1064	1062	$\nu_{\text{asy}}(\text{C-O})$
	978	975	$\delta(\text{C-H})$
931			$\nu(\text{O-H})$
	859	854	$\delta(\text{C-H})$
664	680	660	$\nu(\text{C-S})$

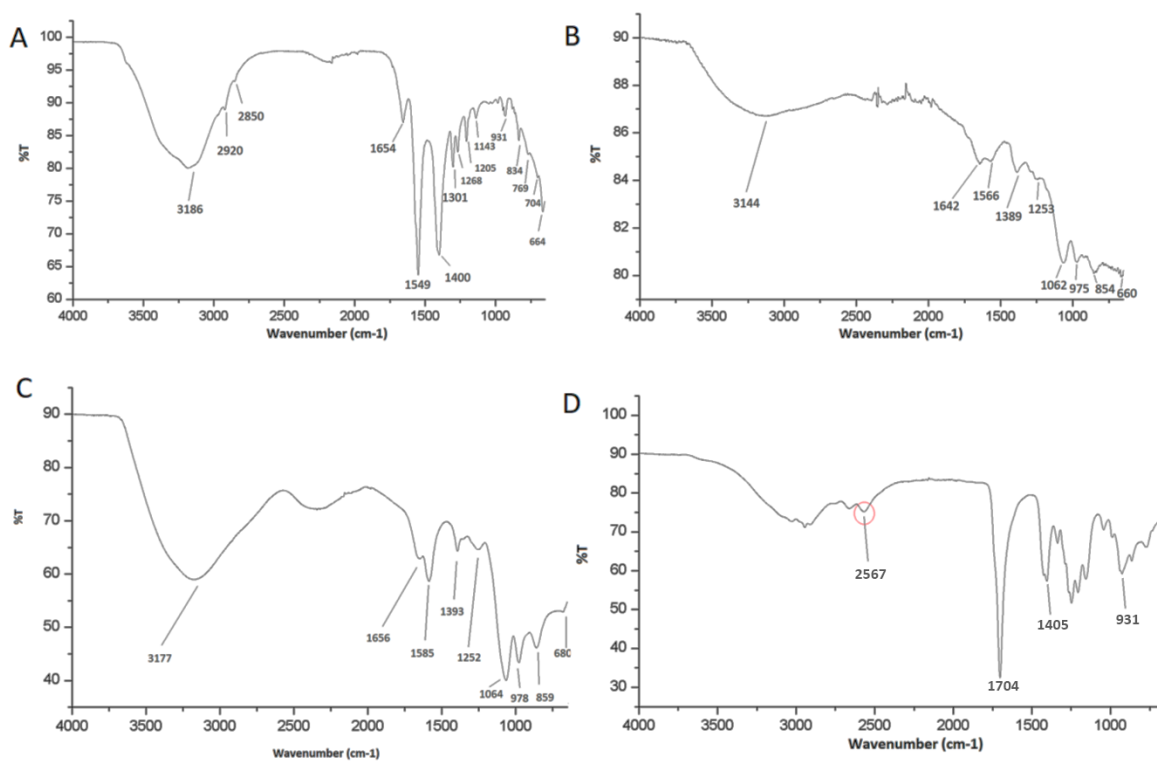


Figure S13. ATR-FTIR spectra of A) 3-MPA solution (pH 10.95), B) 3-MPA-AuNP purchased, C) 3-MPA-AuNP synthesized, and D) 3-MPA solution (pH 4.1).

The peak assignments for the L-selenocystine containing samples are presented in Table 5.

ATR-FTIR data for the respective functionalized samples are depicted in Figure S14.

Table S5. Peak identification and comparison of the data obtained by ATR-FTIR analysis for the samples containing L-selenocystine.

Wavenumber (cm ⁻¹)			
L-selenocystine (0.256 mM, pH 10.20)	SeCyst-AuNP synthesized	SeCyst-AuNP purchased	Peak assignment
3345	3201	3188	$\nu(\text{O-H})$
2980		2917	$\nu(\text{C-H})$
		2847	$\nu(\text{C-H})$
	1660	1679	$\nu_{\text{asy}}(\text{COO}^-)$
1572	1590	1546	$\nu(\text{C=O}), \nu(\text{N-H})$
1475	1349	1438	$\delta(\text{C-H})$
1401			$\delta(\text{O-H})$
1292	1262	1261	$\nu(\text{C-N})$
1081	1055	1041	$\nu_{\text{asy}}(\text{C-O})$
	971	969	$\delta(\text{C-H})$
829	843	853	$\delta(\text{C-H})$

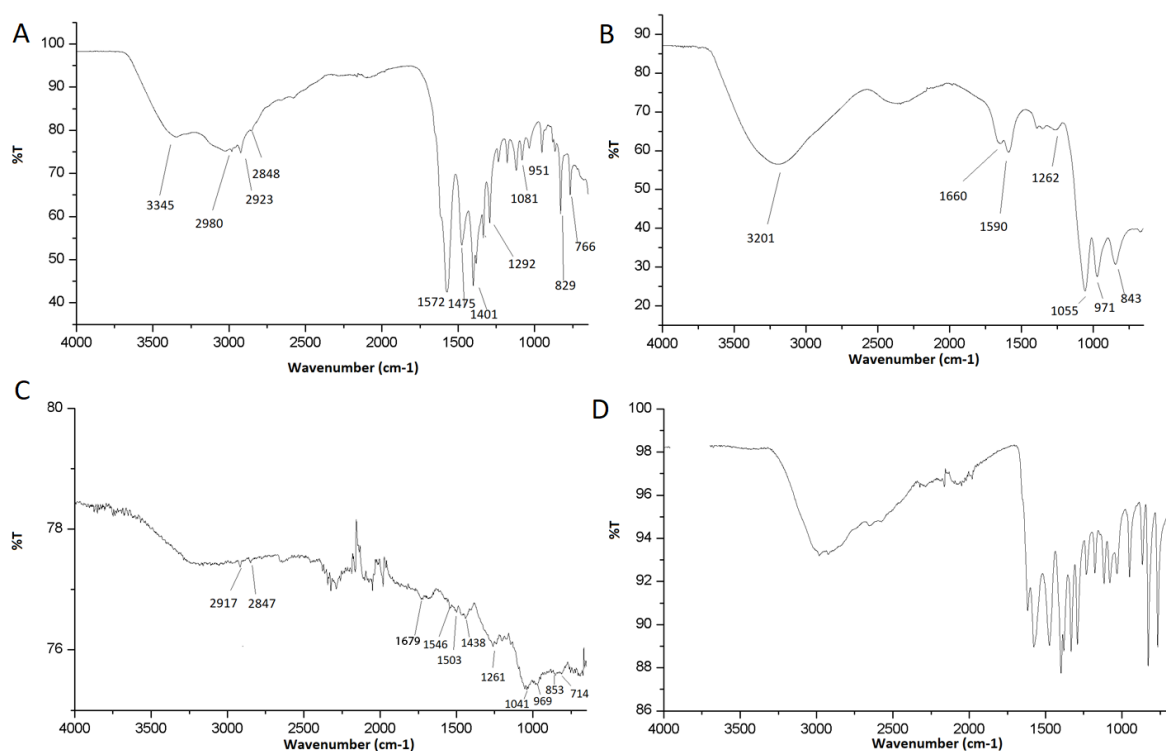


Figure S14. ATR-FTIR spectra of A) L-selenocystine solution (pH 10.20), B) SeCyst-AuNP synthesized, C) SeCyst-AuNP purchased, and D) L-selenocystine solution (pH 9.0).

Characterization of the Capped-AuNPs by TEM

TEM images of purchased (*Figure S15*) and synthesized (*Figure S16*) AuNPs capped with citrate, Cys, 3-MPA and SeCyst.

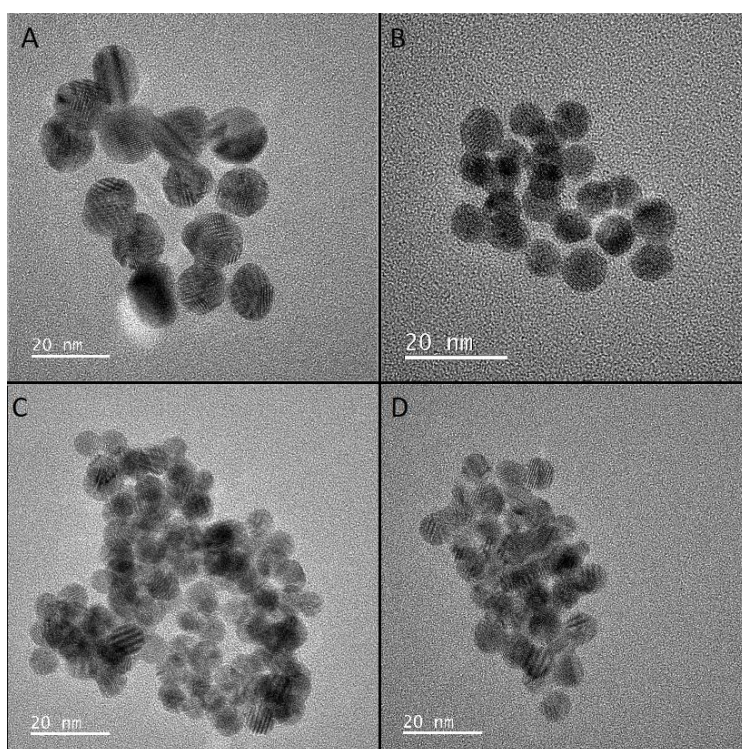


Figure S15. TEM micrograph of A) Cit-AuNPs, B) Cys-AuNPs, C) 3-MPA-AuNPs, and D) SeCyst-AuNPs using purchased nanoparticles.

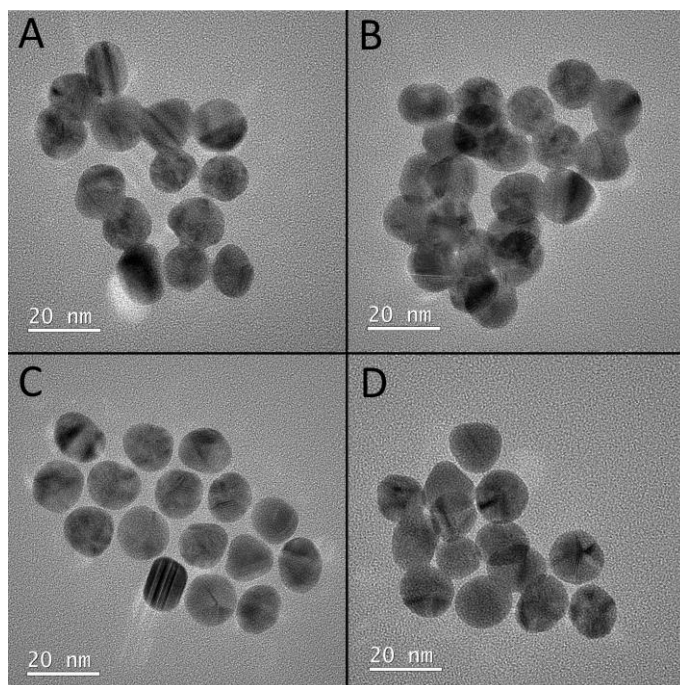


Figure S16. TEM micrograph of A) Cit-AuNPs, B) Cys-AuNPs, C) 3-MPA-AuNPs, and D) SeCyst-AuNPs using the synthesized AuNPs.

In addition, the EDX spectrum from the analyzed area for the synthesized AuNP is shown in Figure S17. Comparing the data obtained from the synthesized Cit-stabilized AuNPs with that of the samples where SeCyst was used as the functionalizing agent (Figure 2), provides confirmation for the successful generation of functionalized SeCyst-AuNPs, due to the absence of the Se peaks in the former.

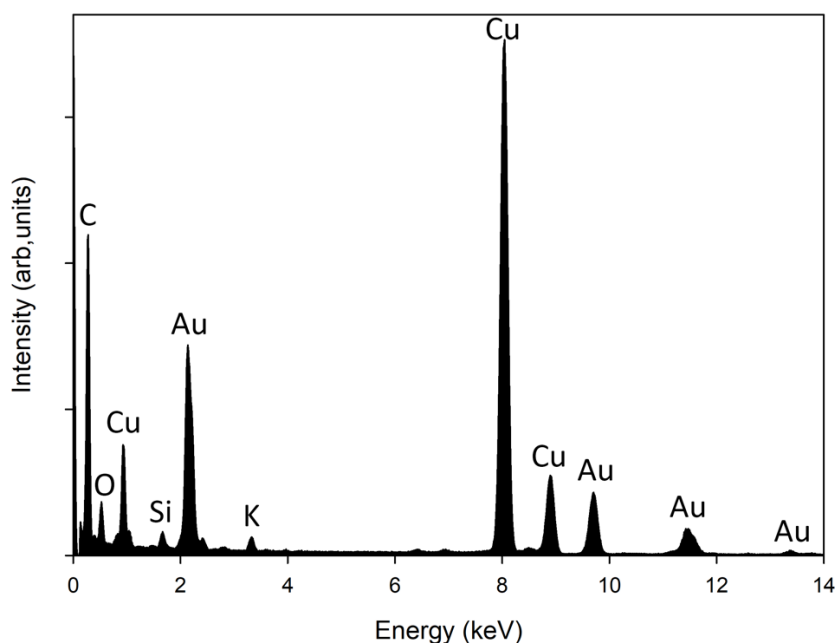


Figure S17. EDX spectrum from the analyzed area of the synthesized AuNPs with the Au $M\alpha$ signals identified (C, O, Si and Cu may be from the supporting TEM grid and carbon film, while K signal may be from external contamination).

EDX maps and spectra from the analyzed area for the purchased AuNPs and SeCyst-AuNPs are demonstrated in Figure S18. The profile of the spectrum belonging to SeCyst-AuNPs compared to the purchased citrate stabilized AuNPs shows the presence of Se in the sample, thus confirming the successful functionalization with SeCyst. Furthermore, EDX mapping of the Au and Se regions indicates that these signals were overlapping (Figure S18B).

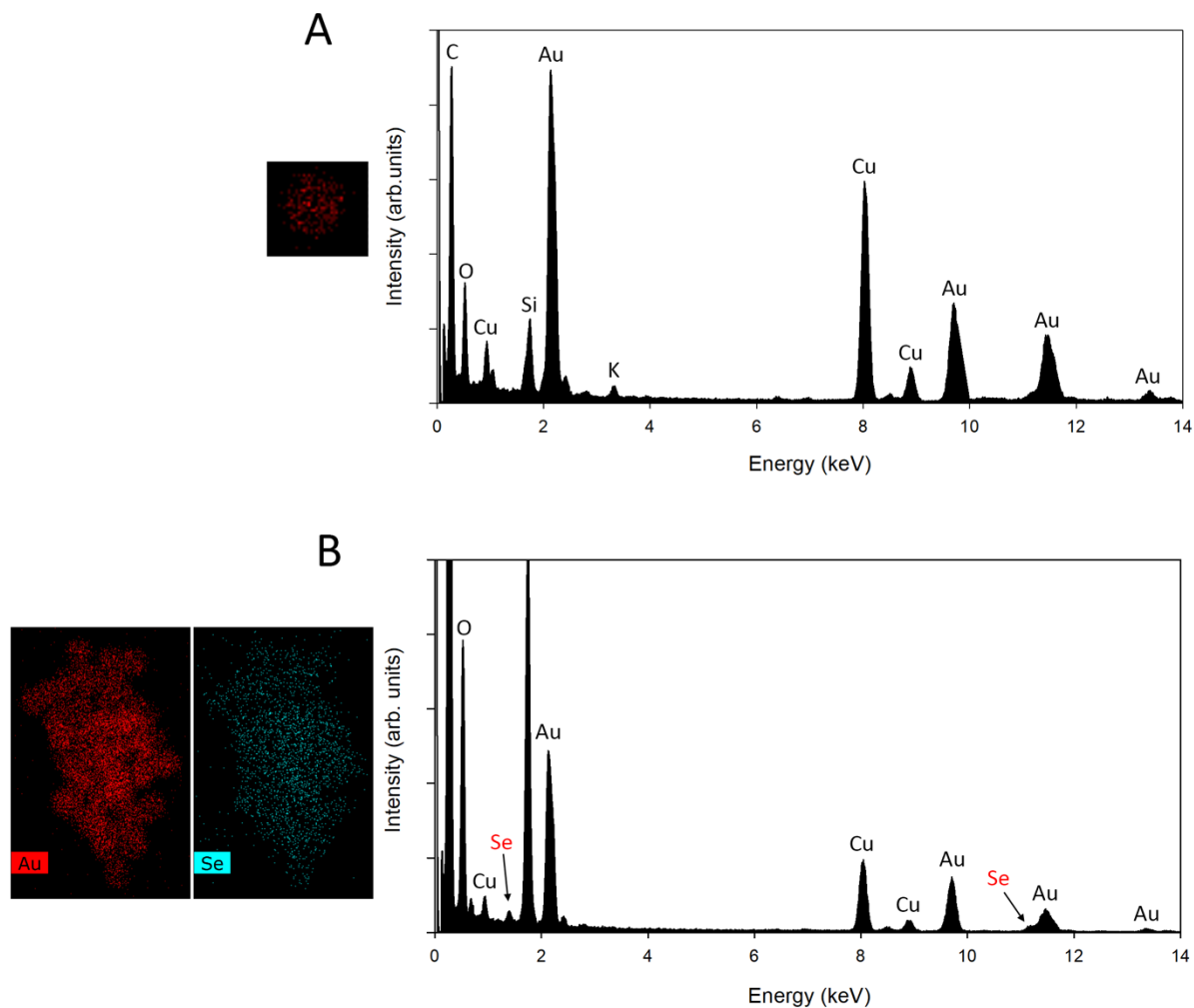


Figure S18. Analysis of SeCyst-AuNPs using the purchased nanoparticles, confirming the successful functionalization with SeCyst. A) Au EDX map on the left side and EDX spectrum of the purchased AuNPs. B) Au and Se EDX map on the left side and EDX spectrum from the analyzed area, with both $M\alpha$ and $Se\ L\alpha$ signals (C, O, Si and Cu may be from the supporting TEM grid and carbon film).

Optimization of the Purification Conditions of the Functionalized AuNPs

In order to optimize the experimental conditions for the purification of the capped gold nanoparticles, a range of different speeds and centrifugation durations were investigated. The aim was to find a combination of conditions under which both the excess functionalizing agents and citrate were removed, and the resultant pellets were easily dispersed. All reactions were carried out at 4 °C. Five different procedures were tested, as follows: 1) centrifugation at 12,000 g for 20 min, 2) centrifugation at 13,200 g for 20 min, 3) centrifugation at 15,800 g for 20 min, 4) centrifugation at 15,800 g for 1 h, 5) centrifugation at 13,200 g for 40 min. In the first three procedures, the supernatant remained pink, indicating the incomplete sedimentation of the NPs. The conditions used in the fourth procedure resulted in the formation of tightly packed pellets on the tube walls, a phenomenon that has been previously described.¹ However, the fifth combination of centrifugation

force and duration gave a colourless supernatant with loose pink pellet at the bottom of the tube. This process was performed three times in order to purify the functionalized AuNPs. The sample pellet was sonicated between each centrifugation step to enable resuspension of the AuNPs into solution. For the washes, phosphate buffer (pH 7.7) was used after the first round of centrifugation, to lower the pH after the functionalization has taken place. The second wash was done using D₂O, to remove any remaining deionized H₂O. During preliminary studies, it was observed that the use of deionized water as solvent was causing interferences in the ¹H-NMR and ATR-FTIR measurements, by masking important peaks. Therefore, D₂O was considered an appropriate substitute for deionized water, as it was demonstrated that in the presence of D₂O no variations in the SPR bands were observed.

In initial experiments, higher concentration values of Cys (between 0.256-5.06 M) were employed to produce Cys-AuNPs (SAMs), using either D₂O or deionized water as solvents. Apart from the highest ratio of 10000:1, that is at a concentration of 5.06 M of Cys, where aggregation of the particles had occurred with complete abolition of the SPR band of the AuNPs, the D₂O-based samples displayed an overall better stability compared to the respective H₂O-based (*Figure S19*). In D₂O the interactions between the amine and carboxyl groups on neighbouring AuNPs are weak hence aggregation is prevented. In contrast, aggregation of the particles occurred, beginning at the lowest ratios when Cys was dissolved in deionized water. Thus, the stability of the AuNPs in D₂O is noteworthy, especially in the presence of high concentrations of Cys. ¹H NMR measurements on the samples were not sensitive enough to provide evidence of the functionalization of the AuNPs.

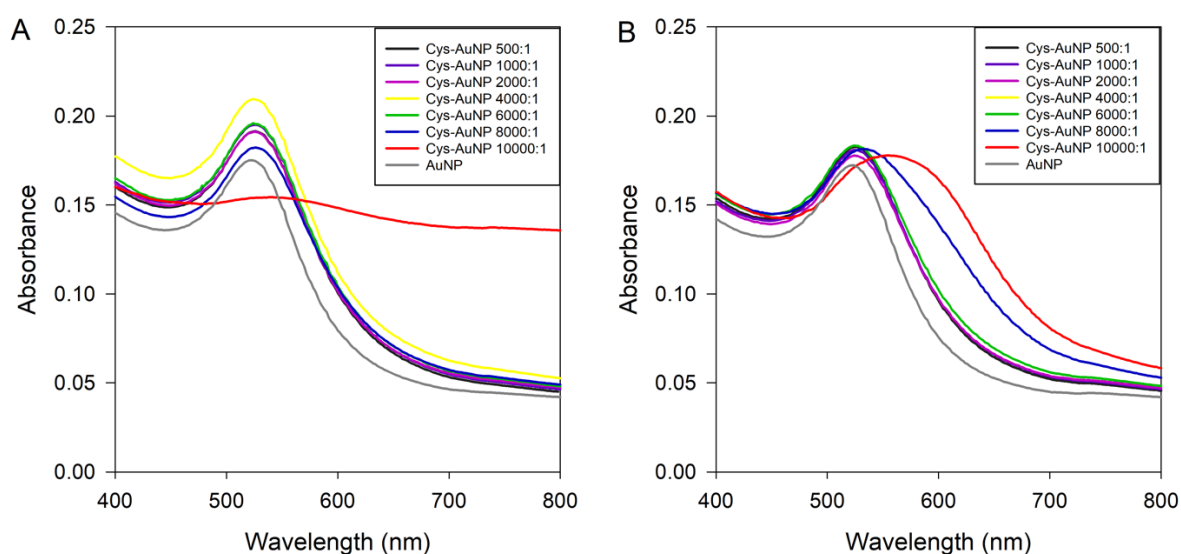


Figure S19. UV-vis spectra for stability assessment of Cys-AuNPs A) in D₂O, and B) in deionized water at high concentrations (0.256-5.06 M).

References

1. Balasubramanian, S.K.; Yang, L.; Yung, L.Y.L.; Ong, C.N.; Ong, W.Y.; Yu, L.E. Characterization, purification, and stability of gold nanoparticles. *Biomaterials* **2010**, *31*, 9023–9030.